NUMERICAL AND ANALYTICAL STUDIES OF MATCHED KINETIC QUASI-EQUILIBRIUM SOLUTIONS FOR AN INTENSE CHARGED PARTICLE BEAM PROPAGATING THROUGH A PERIODIC FOCUSING QUADRUPOLE LATTICE*

Edward A. Startsev, Ronald C. Davidson and Mikhail Dorf
Plasma Physics Laboratory, Princeton University, Princeton, New Jersey, USA

Abstract

A recently developed novel perturbative Hamiltonian transformation method which allows the determination of approximate matched kinetic quasi-equilibrium solutions for an intense charged particle beam propagating through a periodic focusing quadrupole lattice is presented [1]. Using this method we have identified numerically the class of self-consistent periodic kinetic 'equilibria' for intense beam propagation in alternating-gradient focusing systems, and extended the nonlinear perturbative particle simulation method to intense beam propagation in such systems. The new method has been implemented in the nonlinear perturbative particle-in-cell code BEST which is used to study properties of the newly constructed beam 'equilibria'. The results of these studies are presented and analyzed in detail.

INTRODUCTION

Identifying regimes for quiescent beam propagation has been one of the main challenges of accelerator research [2]. In particular, the development of systematic approaches that are able to treat self-consistently the applied periodic focusing force and the self-field force of the beam particles simultaneously is very important [3]. Several recent investigations [4, 5, 6] have used standard Hamiltonian perturbative methods which have turned out to be cumbersome. Recently we have developed [1] a powerful Hamiltonian technique which avoids many of the problems encountered in previous formulations. An advantage of this new approach is that instead of using a generating function that is a function of the mixed set of variables, we work with functions that depend exclusively on a new non-oscillating set of variables from the outset. This significantly simplifies the analysis, and allows the development of an iterative procedure that makes no reference to the generating function in its final form. This approach also provides a more consistent ordering of all relevant quantities in the derivation of the canonical transformation, and provides a simple way to include the beam space-charge effects in the analysis. In this new ordering, all quantifies are expanded in the small parameter $\bar{\epsilon} \sim \sigma_v/2\pi$, where σ_v is the vacuum phase advance. The well-known smooth-focusing approximation for intense charged particle beams appears as the result of first-order expansion in the small parameter $\bar{\epsilon} \sim \sigma_v/2\pi$. Before this work, it was not known how the next order corrections scale with the beam intensity and the small parameter $\bar{\epsilon} \sim \sigma_v/2\pi$. Using the new approach, we have shown that the corrections to the smooth-focusing approximation for intense charged particle beams scale as $\sim (\sigma_v/2\pi)^2$. We have also derived the limits on beam intensity for which the lowest order smooth focusing approximation fails.

* Research supported by the U. S. Department of Energy.

PERTURBATIVE HAMILTONIAN TRANSFORMATION METHOD

The transverse dynamics of a coasting intense charged particle beam inside an alternating-gradient focussing channel with externally applied, transverse focusing force with components $F^{\alpha}_{foc} = -\kappa(s)\eta^{\alpha}x^{\alpha}$, where $\kappa(s)$ is the focusing field strength, and $\eta^1 = 1, \eta^2 = -1$, can be described by the nonlinear Vlasov-Poisson system of equations for the beam distribution function $f(x, p, s)$ and the normalized self-field potential $\Psi(x, s)$ [1]. Here, $s = v_b t$ is the longitudinal coordinate, where $v_b = const.$ is the directed beam velocity. Moreover, we use an index notation where $(x, y) \equiv (x^1, x^2)$, and $(p_x, p_y) \equiv (p^1, p^2)$. For simplicity, we also suppress variable indices inside function definitions, i.e., we employ the notation $f(x^1, x^2, p^1, p^2, s) \equiv f(x, p, s)$ and $\Psi(x^1, x^2, s) \equiv \Psi(x, s)$. It is convenient to introduce the dimensionless re-normalized variables $\bar{x} = x/a$, $\bar{s} = s/S$, $\bar{\kappa}(\bar{s}) = \kappa(s)/\kappa_0$, $\bar{p} = p/(a\kappa_0 S)$ and $\bar{f} = (f/N)a^4(\kappa_0 S)^2$, where S is the period of the applied focusing lattice, a is the characteristic transverse beam dimension, and κ_0 is the characteristic value of the lattice function $\kappa(s)$. Here we also specialize to the case of a periodic lattice with *odd* half-lattice-period symmetry, $\kappa(s) = -\kappa(s + S/2)$.

Dropping the bar notation over the normalized variables, the distribution function $f(x, p, s)$ satisfies the nonlinear Vlasov equation [1]

$$\frac{df}{ds} = \frac{\partial f}{\partial s} + \sum_{\alpha=1}^{2} \frac{dx^{\alpha}}{ds}\frac{\partial f}{\partial x^{\alpha}} + \sum_{\alpha=1}^{2} \frac{dp^{\alpha}}{ds}\frac{\partial f}{\partial p^{\alpha}} = 0, \quad (1)$$

where

$$\frac{dx^{\alpha}}{ds} = \frac{\partial H}{\partial p^{\alpha}}, \quad \frac{dp^{\alpha}}{ds} = -\frac{\partial H}{\partial x^{\alpha}}, \quad (2)$$

are the particle equations of motion. The Hamiltonian $H(x, p, s)$ is defined by

$$H(x, p, s) = \kappa(s)\frac{[\eta^{\alpha}x^{\alpha}x^{\alpha}]}{2} + \epsilon\Big\{\frac{[p^{\alpha}p^{\alpha}]}{2} + \\ + \int L(x, x')f(x', p', s)Dx'Dp'\Big\}. \quad (3)$$

For simplicity, we adopt a square-bracket notation for summations, e.g., $[x^\alpha x^\alpha] \equiv \sum_{\alpha=1}^{2} x^\alpha x^\alpha$. Moreover, for multi-dimensional integrals, we adopt the notation $\int dx_1 dx_2 Z = \int DxZ$. In Eq. (3), ϵ is defined by $\epsilon \equiv S^2\kappa_0$, and the Green's function $L(x, x')$ satisfies the equation

$$\left[\frac{\partial}{\partial x^\alpha}\frac{\partial}{\partial x^\alpha}\right] L(x, x') = -s_b\delta(x - x'). \tag{4}$$

Here, $s_b = 2\pi A/(\kappa_0 S)^2 a^2 = (4\pi q^2 N/m_b a^2\gamma_b^3)/(\kappa_0 S v_b)^2$ is a dimensionless measure of the beam space-charge intensity. For a beam transversely confined by the external focusing lattice, the characteristic maximum value of the normalized intensity s_b is $(s_b)^{max} \sim 1$. In Eq. (3), the function f is normalized according to $\int dxdpf = 1$. In our recent study [1] we examined the matched quasi-equilibrium solutions to the Vlasov equation (1) by searching for a time-dependent canonical transformation of the form [1, 4, 5, 6] $(x^\alpha, p^\alpha, H, s) \to (Q^\alpha, P^\alpha, K, s)$, where

$$x^\alpha = x^\alpha(Q, P, s), \quad p^\alpha = p^\alpha(Q, P, s), \tag{5}$$

with *time-independent* transformed Hamiltonian $K(Q, P)$. Here we briefly summarize the results. For every canonical transformation there is a function $\tilde{S}$ that satisfies the differential relation

$$[p^\alpha dx^\alpha] - Hds = d\tilde{S} + [P^\alpha dQ^\alpha] - Kds. \tag{6}$$

The relationships between the old and new set of phase-space coordinates are obtained from Eq. (6) by equating coefficients in front of the differentials of the independent variables $(dP^\alpha, dQ^\alpha, ds)$.

Following the procedure outlined in Ref. [1], we express

$$\begin{aligned} p &= p_0(Q, P, s) + \sum_{n=1}^{\infty}\epsilon^n p_n, \quad x = Q + \sum_{n=1}^{\infty}\epsilon^n x_n, \\ S &= S_0(Q, P, s) + \sum_{n=1}^{\infty}\epsilon^n S_n, \\ K &= K_0(Q, P) + \sum_{n=1}^{\infty}\epsilon^n K_n, \end{aligned} \tag{7}$$

where $p_n(Q, P, s)$, $x_n(Q, P, s)$, $S_n(Q, P, s)$ and $K_n(Q, P)$ $(n = 0, 1, 2, \cdots)$ are functions to be determined from the iterative procedure. Using Eq. (7), we expand the Hamiltonian H in Eq. (3) according to

$$H(x, p, s) = \sum_{n=0}^{\infty}\epsilon^n H_n(Q, P, s). \tag{8}$$

Solving iteratively to the second order in ϵ, we obtains the canonical transformations

$$\begin{aligned} x^\alpha &= Q^\alpha - \epsilon\kappa^{(2)}\eta^\alpha Q^\alpha \\ &+\epsilon^2\left\{2\kappa^{(3)}\eta^\alpha P^\alpha + (\kappa\kappa^{(2)})^{(2)}Q^\alpha\right\}, \end{aligned} \tag{9}$$

and

$$\begin{aligned} p^\alpha &= \left\{P^\alpha - \kappa^{(1)}\eta^\alpha Q^\alpha\right\} \\ &+\epsilon\left\{\kappa^{(2)}\eta^\alpha P^\alpha + (\kappa\kappa^{(2)})^{(1)}Q^\alpha\right\} + \\ &+\epsilon^2\left\{\left(3 < (\kappa^{(2)})^2 > -2(\kappa\kappa^{(3)})^{(1)} - (\kappa\kappa^{(2)})^{(2)}\right)P^\alpha\right. \\ &\left.+\left(\kappa^{(3)} < (\kappa^{(1)})^2 > -(\kappa(\kappa\kappa^{(2)})^{(2)})^{(1)}\right)\eta^\alpha Q^\alpha\right\} \\ &+\epsilon\frac{\partial}{\partial Q^\alpha}\Psi(Q)^{(1)}. \end{aligned} \tag{10}$$

Here, $< A >\equiv (1/S)\int_s^{s+S} d\bar{s}A(\bar{s})$, and $\ll A \gg \equiv A - < A >$. Here, we also introduce the notation $A^{(0)} \equiv \ll A \gg$ and

$$A^{(n)} \equiv \ll \int dsA^{(n-1)} \gg \tag{11}$$

for $n \geq 1$. The time-independent Hamiltonian is then determined to be [correct to the third order in ϵ, since one ϵ re-normalizes time, so that transformed quantities are slow functions of time, i.e., $Q(\epsilon s)$]

$$\begin{aligned} K = \epsilon\Bigg\{&\frac{[P^\alpha P^\alpha]}{2}\left(1 + 3\epsilon^2 < (\kappa^{(2)})^2 >\right) \\ &+\frac{[Q^\alpha Q^\alpha]}{2}\left(< (\kappa^{(1)})^2 > +\epsilon^2 < ((\kappa\kappa^{(2)})^{(1)})^2 >\right) \\ &+ < \Psi(Q) > \Bigg\} \end{aligned} \tag{12}$$

In Eqs. (9)–(12), the function $\Psi(Q)$ is defined correct to second order in ϵ as

$$\begin{aligned} &\Psi(Q) = \\ &\int D\bar{Q}L(Q_\alpha(1 + \epsilon\eta^\alpha\kappa^{(2)}), \bar{Q}_\alpha(1 + \epsilon\eta^\alpha\kappa^{(2)}))n(\bar{Q}), \end{aligned} \tag{13}$$

where $n(Q) = \int DPF(Q, P)$. The case with distribution function in slow variables $F(Q, P)$, which is independent of time, corresponds to a beam which is matched to the lattice, with all beam quantities changing periodically with time $f(x, p, s + S) = f(x, p, s)$. Note from Eqs. (9)–(12) and the definitions in Eq. (11), that the actual expansion parameter in Eqs. (9)–(12) is not ϵ, but rather $\bar{\epsilon} \equiv \epsilon[< (\kappa^{(1)})^2 >]^{1/2} \sim \sigma_v/(2\pi)$. For a lattice with small filling factor $\delta \sim T/S \ll 1$, when the focusing elements occupy a distance $2T$ which a small portion of the lattice period S, the correction $[< (\kappa^{(1)})^2 >]^{1/2} \sim \delta$ can be important. For such lattices the theory presented in this paper still applies even if $\epsilon > 1$, provided the condition $\epsilon\delta \ll 1$ still holds.

In Ref. [1] we obtained the expressions for $< \Psi(Q) >$ correct to the second order in ϵ for arbitrary boundary conditions. Here we study in more details the particular case of a thermal equilibrium distribution, i.e.,

$$F(Q, P) = \frac{\bar{n}[1 + 3\epsilon^2 < (\kappa^{(2)})^2 >]}{2\pi T}\exp\left(-\frac{K(Q, P)/\epsilon}{T}\right), \tag{14}$$

where T is the normalized temperature, and $\bar{n}$ is the normalized on-axis density. We aslo specialize to the case where the boundary is removed far away from the beam. In cylindrical coordinates (r,θ) where $Q^1 = r\cos(\theta)$ and $Q^2 = r\sin(\theta)$, the averaged potential can be expressed as $< \Psi >= \Phi_0(r) + \epsilon^2 < (\kappa^{(2)})^2 > \cos(4\theta)q(r)$. By introducing the re-normalized distance $\rho^2 = r^2 s_b \bar{n}/T$ and re-normalized potentials $\bar{\phi}_0 = \Phi_0/T$, $\bar{q} = q/T$, and beam intensity parameter $\bar{s} = s_b\bar{n}/(2k^2)$, the equation determining the normalized potentials can be rewritten as

$$\left(\frac{1}{\rho}\frac{d}{d\rho}\rho\frac{d}{d\rho} - \frac{16}{\rho^2} - \bar{n}_0(\rho)\right)\bar{q}(r) = \qquad (15)$$
$$-2\left(\bar{n}_0 + \frac{4}{\rho^2}\int_0^\rho d\rho\overline{\rho n}_0(\bar{\rho}) - \frac{12}{\rho^4}\int_0^\rho d\rho\overline{\rho^3}\bar{n}_0(\bar{\rho})\right),$$

with boundary conditions

$$\bar{q}(\infty) = \frac{1}{2}\int_0^\infty d\rho\overline{\rho n}_0(\bar{\rho}), \quad \bar{q}(0) = 0, \qquad (16)$$

where the zero-order normalized density profile $\bar{n}_0 = n_0/\bar{n} = \exp(-\rho^2/4\bar{s} - \bar{\phi}_0)$ satisfies the nonlinear equation

$$\frac{1}{\rho}\frac{d}{d\rho}\rho\frac{d}{d\rho}\bar{n}_0 + \bar{n}_0\left(\frac{1}{\bar{s}} - \bar{n}_0\right) - \frac{(\bar{n}_0')^2}{\bar{n}_0} = 0. \qquad (17)$$

Note that the solutions of Eqs. (15)-(17) depend only on the dimensionless beam intensity parameter $\bar{s}$.

Making use of the above definitions, the normalized equilibrium density profile, accurate to second order in ϵ, can be expressed as

$$\bar{n}(\rho,\theta) = \bar{n}_0(\rho)[1 - \epsilon^2 < (\kappa^{(2)})^2 > \cos(4\theta)\bar{q}(\rho)]. \qquad (18)$$

Next, we introduce the RMS radius $\rho_{rms}(\theta)$, defined separately for each azimuthal angle θ as

$$\rho_{rms}^2(\theta) \equiv \frac{\int_0^\infty d\rho\rho^3\bar{n}(\rho,\theta)}{\int_0^\infty d\rho\rho\bar{n}(\rho,\theta)}. \qquad (19)$$

Using Eq. (18), the relative change in the RMS beam radius as function of angle θ can be expressed as

$$\delta\rho_{rms}(\theta)/\rho_{rms}^0 = -\epsilon^2 < (\kappa^{(2)})^2 > \cos(4\theta)A(\bar{s}), \qquad (20)$$

where the function $A(\bar{s})$ is given by

$$A(\bar{s}) = \frac{1}{2}\left(\frac{\int_0^\infty d\rho\rho^3\bar{n}_0(\rho)\bar{q}(\rho)}{\int_0^\infty d\rho\rho^3\bar{n}_0(\rho)} - \frac{\int_0^\infty d\rho\rho\bar{n}_0(\rho)\bar{q}(\rho)}{\int_0^\infty d\rho\rho\bar{n}_0(\rho)}\right). \qquad (21)$$

Equation (17) for the density profile $\bar{n}_0$ has been analyzed in Ref. [7]. There, it was shown that the solution satisfying the boundary conditions $\bar{n}_0(0) = 1$ and $\bar{n}_0(\infty) = 0$ exists only for values of beam intensity parameter $\bar{s} < 1$. For low-intensity beams, $\bar{s} \ll 1$, the solution can be approximated by

$$\bar{n}_0(\rho) \approx \left(1 + \frac{\rho^2}{4\bar{s}}\right)^{\bar{s}}\exp\left(-\frac{\rho^2}{4\bar{s}}\right), \qquad (22)$$

and for high-intensity beams with $\Delta \equiv 1/\bar{s} - 1 \ll 1$ the solution can be approximated by

$$\bar{n}_0(\rho) \approx \frac{\left[1 + \frac{1}{2}\Delta + \frac{1}{24}\Delta^2\right]^2}{\left[1 + \frac{1}{2}\Delta I_0(\rho) + \frac{1}{24}[\Delta I_0(\rho)]^2\right]^2}, \qquad (23)$$

where $I_0(\rho)$ is the modified Bessel function of zero order. The beam density profiles $\bar{n}_0(\rho)$ obtained by numerical integration of Eq. (17) are plotted in Fig. 1 for several values of the beam intensity parameter $\bar{s}$ and compared with the approximate expressions in Eqs. (22) and (23). These density profiles have been used to numerically integrate Eq. (15), and the results are illustrated in Fig. 2, where the function $\bar{n}_0(\rho)\bar{q}(\rho)$, which is the radial profile of the perturbation in the density profile [Eq. (18)], is plotted for different values of the intensity parameter $\bar{s} = 0.3; 0.6; 0.9; 0.99; 0.999$.

The function $A(\bar{s})$, which determines the intensity dependence of the angle-dependent corrections [see Eq.(20)], is plotted in Fig. 3.

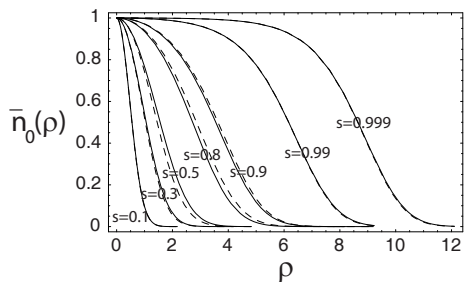

Figure 1: Plots of density profiles $\bar{n}_0(\rho)$ for different values of the intensity parameter $\bar{s} = 0.1; 0.3; 0.5; 0.8; 0.9; 0.99; 0.999$. The solid lines correspond to the numerical solutions of Eq. (17). The dashed lines correspond to the approximate expressions in Eq. (22) for $\bar{s} = 0.1; 0.3; 0.5$, and in Eq. (23) for $\bar{s} = 0.8; 0.9; 0.99; 0.999$.

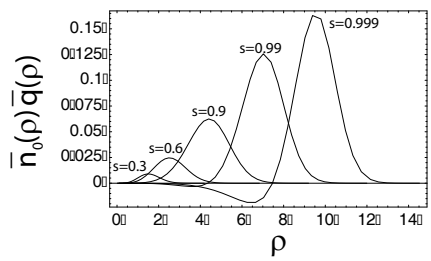

Figure 2: Plots of $\bar{q}(\rho)\bar{n}_0(\rho)$ for different values of the intensity parameter $\bar{s} = 0.3; 0.6; 0.9; 0.99; 0.999$ obtained from numerical solutions to Eqs. (15) and (16).

SIMULATION STUDIES

To study corrections to zero-order smooth-focusing approximation we have used the nonlinear δf particle-in-cell

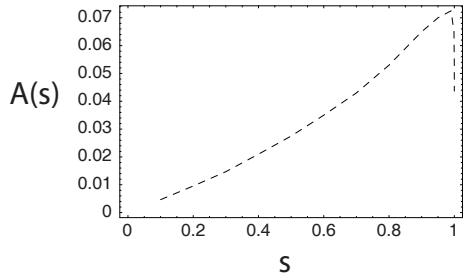

Figure 3: Plots of the function $A(\bar{s})$ in Eq. (21).

code BEST [8]. The δf code is ideally suited for this purpose due its low noise and ability to resolve small perturbations around the approximately known quasi-equilibrium beam state. The BEST code has been modified to simulate the beam inside the alternating-gradient focusing-defocusing channel with externally applied, transverse focusing force with components $F^{\alpha}_{foc} = -\kappa(s)\eta^{\alpha}x^{\alpha}$, where $\kappa(s)$ is the focusing field strength.

At every time-step of the simulations each beam particle has phase-space coordinates (x, p) and approximate non-oscillating coordinates $(\bar{Q}, \bar{P})$ which are related to (x, p) by Eqs. (9)-(10) with terms proportional to the self-field correction [the oscillating term $\epsilon\frac{\partial}{\partial Q^{\alpha}}\Psi(Q)^{(1)}$ in the the equation for P^{α}] neglected. This determines the linear transformation matrix $\hat{A}(s)$ as

$$\begin{pmatrix} \bar{Q} \\ \bar{P} \end{pmatrix}^{\alpha} = \hat{A}^{\alpha}(s)\begin{pmatrix} x \\ p \end{pmatrix}^{\alpha} \tag{24}$$

The initial time is chosen so that the correction term $\epsilon\frac{\partial}{\partial Q^{\alpha}}\Psi(Q)^{(1)} = 0$ at $s = 0$ and the transformation in Eq. (24) is exact up to second order in ϵ at this time. Each particle also carries the approximate average energy $\bar{K}$ calculated using Eq. (14) but with approximate non-oscillating phase-space coordinates $(\bar{Q}, \bar{P})$ given by Eq. (24). This introduces a purely oscillating second-order error $\delta K = K - \bar{K} = \epsilon[P^{\alpha}\frac{\partial}{\partial Q^{\alpha}}\Psi(Q)^{(1)}]$ in the calculated value of the average energy $\bar{K}$. The second-order corrections to the self-field potential are also are not used in calculating $\bar{K}$.

The loading of the charged particle beam in the beginning of the simulation is done in slow phase-space coordinates $(\bar{P}, \bar{Q})$ with a thermal equilibrium distribution given by Eq. (14), but without terms proportional to the second-order self-field correction to the average self-field potential $< \Phi(Q) >$ in the equation for the average Hamiltonian K in Eq. (12)]. The resulting initial distribution F_0 is different from the quasi-equilibrium distribution F given by Eq. (14) by a non-oscillating term $< \delta F >= F_0(< \Psi > -\Phi_0)/T$ which is due to the neglected term in the equation for K.

After the initial loading, the unaveraged beam particle phase-space coordinates (x, p) are advanced in time using Hamiltonian Eqs. (2) with self-field potential in Eq. (3) determined as follows. At every times step the particle distribution is given by a distribution function which can be expressed either in fast (x, p) or slow $(\bar{Q}, \bar{P})$ phase-space variables $f(x, p, s) = G(\bar{Q}, \bar{P}, s) = F_0(\bar{Q}, \bar{P}) + w(\bar{P}, \bar{Q}, s)G(\bar{Q}, \bar{P}, s)$. This is because $det\hat{A}(s) = 1$ and we have introduced the weight function $w(\bar{P}, \bar{Q}, s)$. From $df/ds = 0$ and $dF_0(\bar{P}, \bar{Q})/ds = -(F_0/T)d\bar{K}/ds$ we obtain the equation for the weight function w

$$\frac{dw}{ds} = \frac{(1-w)}{T}\frac{d\bar{K}}{ds}, \tag{25}$$

where

$$\frac{d\bar{K}}{ds} = \frac{\partial\bar{K}}{\partial\bar{Q}}\frac{d\bar{Q}}{ds} + \frac{\partial\bar{K}}{\partial\bar{P}}\frac{d\bar{P}}{ds}. \tag{26}$$

The coefficients $\partial\bar{K}/\partial\bar{Q}$ and $\partial\bar{K}/\partial\bar{P}$ are calculated from the definition of $\bar{K}(\bar{Q}, \bar{P})$, while $d\bar{Q}/ds$ and $d\bar{P}/ds$ are obtained from differentiation of Eq. (24) and use of the Hamiltonian equations (2).

To calculate the self-field forces acting on the beam particle we need to calculate the unaveraged self-field potential $\phi(x)$. To do that we first calculate the unaveraged beam density as

$$\begin{aligned} n(x) &= \int D\bar{P}D\bar{Q}F_0(\bar{P}, \bar{Q})\delta[x - x(\bar{Q}, \bar{P})] \\ &+ \int D\bar{P}D\bar{Q}w(\bar{P}, \bar{Q}, s)G(\bar{P}, \bar{Q}, s)\delta[x - x(\bar{Q}, \bar{P})] = \\ &(A^1_{11}A^2_{11})n_0[A_{11}(s)x] \\ &+ \int D\bar{P}D\bar{Q}wG\delta(x - x(\bar{Q}, \bar{P}), \end{aligned} \tag{27}$$

where we have approximated $Q^{\alpha} = A^{\alpha}_{11}(s)x^{\alpha}$, which introduces a purely oscillating error $\sim \epsilon^2$ in approximating the first integral in Eq. (27). Next, the unaveraged potential is calculated by solving the Poisson equation $\nabla^2\phi(x) = -s_b n(x)$.

The statistical errors in the simulations which employ this scheme are reduced significantly by a factor $\sim (< w^2 >)^{(1/2)}$ [8] compared to regular particle-in-cell simulations.

Because the initial distribution differs from the quasi-equilibrium distribution by a factor $\sim \epsilon^2$, the average particle weight is proportional to $\sim (< w^2 >)^{(1/2)} \sim \epsilon^2$ during the simulation. Because we introduced a purely oscillating error $\sim \epsilon^2$ in the calculation of the self-field, we can only determine correct up to second order in ϵ the average quantities in the final state of the simulation when the initial transients have damped out. To calculate the average quantities correct up to the second order we can use the approximate slow phase-space coordinates $(\bar{Q}, \bar{P})$, since the second-order errors introduced by the use of this approximation will be purely oscillating. For example, we can determine the second-order corrections to the quasi-equilibrium density profile given by Eq. (18) by calculating the particle density in $\bar{Q}$ space weighted by the weight function w. The result can be used to evaluate the corrections to the average beam radius from the definition in Eq. (19), and in particular the function $A(\bar{s})$ introduced in Eqs. (20) and (21).

The preliminary results of the simulations are illustrated in Fig. 4-5 for a sinusoidal lattice $\kappa(s) = \kappa_0 \sin(2\pi s/S)$,

with beam parameters: beam intensity $\bar{s} = 0.5$, wall radius $\rho_w = 5\rho^0_{rms}$, and $\sigma_v = 25^0$ which corresponds to $\epsilon = 0.07$. In Fig. 4 the Fourier spectrum $\sim exp(im\theta)$ of the averaged over time relative RMS radius change $\delta\rho_{rms}(\theta)/\rho^0_{rms}$ is plotted as a function of azimuthal mode number m. Notice that there are are only $m = 0$ and $m = 4$ components, on average. Fig. 5 shows the time dependence of the $m = 4$ component of $\delta\rho_{rms}(\theta)/\rho^0_{rms}$. Note, that the initial transient is damped out after several betatron oscillations with small-amplitude fast oscillations remaining in the final state. The saturation of the $m = 0$ mode leads to a small beam heating and corresponding profile change, while the $m = 4$ mode saturates at a finite average value. This corresponds to the octupole corrections to the equilibrium beam density profile that have been calculated theoretically and plotted in Figs. 2 and 3.

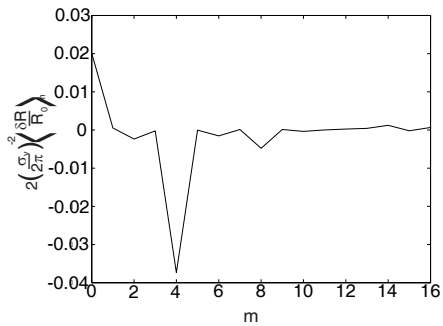

Figure 4: Fourier spectrum $\sim exp(im\theta)$ of the averaged over time relative RMS radius change $\delta\rho_{rms}(\theta)/\rho^0_{rms}$ as a function of azimuthal mode number m.

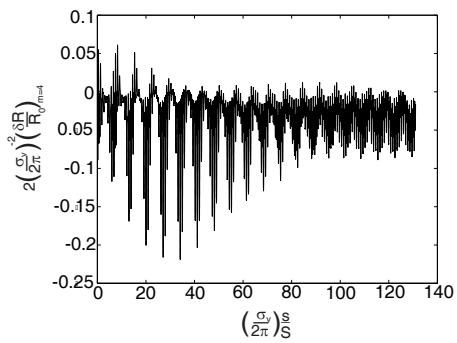

Figure 5: Time history of $m = 4$ component of $\delta\rho_{rms}(\theta)/\rho^0_{rms}$.

CONCLUSIONS

To summarize, we have studied the approximate matched kinetic quasi-equilibrium solutions for an intense charged particle beam propagating through a periodic focusing quadrupole lattice using the recently developed perturbative Hamiltonian transformation method [1]. We have shown that the next-order corrections to the well known smooth-focusing approximation for intense charged particle beams scale as $(\sigma_v/2\pi)^2$, where σ_v is the vacuum phase advance. We have studied the $(\sigma_v/2\pi)^2$ corrections to the beam density profile and have shown that the corrections have octupole structure $\delta n(\rho) \sim -n_0(\rho)\bar{q}(\rho)(\sigma_v/2\pi)^2 cos(4\theta)$ and are localized at the beam edge [see Fig. (1) and (2)]. We have developed the δf particle-in-cell simulation method for determining the corrections numerically. The preliminary results for moderately intense beams with $\bar{s} < 0.6$ confirm the theoretical predictions. The simulations of the highly-tune-depressed beams with $\bar{s} > 0.6$ are now underway. For highly depressed beams with $\bar{s} > 0.6$ the theoretical results for the average self-field potential presented in Eqs. (16)-(17) have to be modified. As obvious from Fig. 1, the zero-order equilibrium density profile develops a sharp gradient at the beam edge at a radius $\rho \sim \rho_{1/2}$, where $n_0(\rho_{1/2}) \equiv 1/2$. At the beam edge $d\Phi_0/d\rho \sim 1$, and therefore the expansion in the small parameter ϵ in Eq. (13) which was used in deriving Eqs. (16)-(17) cannot performed there if $\epsilon\rho_{1/2}(\bar{s}) \sim 1$. As a beam particle performs fast lattice oscillation near the beam edge, it will average out the profile gradient, and the result will yield smaller value for the average self-filed potential. The Equation (13) can still be used to determine the average self-field potential, but the averaging procedure leads to a highly non-local relation between the self-field potential and the average beam particle density. Note, that the corrections to the self-field potential calculated in the smooth-focusing approximation for such intense beams may not be small, and do not scale as $(\sigma_v/2\pi)^2$. Using the approximate expression for beam density profile in Eq. (23) we can obtain the expression for $\rho_{1/2}(\bar{s}) \simeq \ln\left[\frac{C}{\Delta}\sqrt{2\pi\frac{C}{\Delta}}\right]$, where $C \simeq 0.77799$. Therefore, the results presented in Figs. 2-3 are valid for the moderately intense beams with $(\sigma_v/2\pi)\rho_{1/2}(\bar{s}) < 1$.

REFERENCES

[1] E. A. Startsev, R. C. Davidson and M. Dorf, Phys. Rev. ST Accel. Beams **13**, 064402 (2010).

[2] R. C. Davidson, M. Dorf, I. Kaganovich, H. Qin, E. A. Startsev, S. M. Lund, Nucl. Instr. and Meth. in Phys. Res. A **606**, 11 (2009).

[3] E. D. Courant, M. S. Livingstone and H. S. Snyder, Phys. Rev. **88**, 1190 (1952).

[4] P. J. Channell, Phys. Plasmas **6**, 982 (1999).

[5] R. C. Davidson, H. Qin, and P. J. Channell, Phys. Rev. ST Accel. Beams **2**, 074401 (1999); **3**, 029901 (2000).

[6] S. I. Tzenov and R. C. Davidson, Phys. Rev. ST Accel. Beams **5**, 021001 (2002).

[7] E. A. Startsev and S. M. Lund, Phys. Plasmas **15**, 043101 (2008).

[8] E. A. Startsev, R. C. Davidson and H. Qin, Phys. Rev. ST Accel. Beams **8**, 124201 (2005).